

This is the peer reviewed version of the following article: Zhang, Z., Zhu, B., Peng, Z., Yin, R., Baughman, R. H., Tao, X., Programmable and Thermally Hardening Composite Yarn Actuators with a Wide Range of Operating Temperature. *Adv. Mater. Technol.* 2020, 5, 2000329, which has been published in final form at <https://doi.org/10.1002/admt.202000329>. This article may be used for non-commercial purposes in accordance with Wiley Terms and Conditions for Use of Self-Archived Versions. This article may not be enhanced, enriched or otherwise transformed into a derivative work, without express permission from Wiley or by statutory rights under applicable legislation. Copyright notices must not be removed, obscured or modified. The article must be linked to Wiley's version of record on Wiley Online Library and any embedding, framing or otherwise making available the article or pages thereof by third parties from platforms, services and websites other than Wiley Online Library must be prohibited.

Programmable and thermally-hardening composite yarn actuator with a wide range of operating temperature

Ziheng Zhang¹, Bo Zhu², Zehua Peng¹, Rong Yin¹, Ray H. Baughman³, Xiaoming Tao^{1*}

¹ Research Center of Smart Wearable Technology, Institute of Textiles and Clothing
The Hong Kong Polytechnic University, Hong Kong, P. R. China

² College of Professional and Continuing Education, The Hong Kong Polytechnic
University, Hong Kong, P.R. China

³ The Alan G. MacDiarmid NanoTech Institute, The University of Texas at Dallas
Richardson, TX 75080, USA

Corresponding author: xiao-ming.tao@polyu.edu.hk

Abstract

Actuators have wide applications in intelligent robots, deformable textiles and wearable devices, wherein the fiber-based coiled linear actuators are particularly advantageous due to their good flexibility, high stress and strain. However, their performances have been limited by the employed materials, whose microstructures are not easily designed and controlled. This paper proposes a new approach of engineered composite yarns for the actuators. It leads to novel solutions to overcome these difficulties by offering wide design options in material properties and device structures. Here we exemplify an engineering design of programmable and thermally-hardening helical composite yarn actuators (HCYAs) with a wide range of operating temperature. Polyimide (PI) and polydimethylsiloxane (PDMS) were selected to fabricate HCYAs, achieving tensile actuation of 20.7% under 1.2 MPa from -50 °C to 160 °C and competitive specific work (158.9 J/kg, 4 times of natural muscle). With constant tensile deformation, **PI/PDMS** HCYA nearly tripled the stress from 20 °C to 100 °C. Moreover, we surprisingly observed an unusual thermal-hardening phenomenon that the tensile stiffness of the **PI/PDMS** HCYAs increases with the rise of temperature. Equipped by electrothermally powered **PI/Cu/PDMS** HCYAs, robotic hands and pressure-tunable

compressive bandage were demonstrated for their potential applications in robots and wearable devices.

Introduction

Fiber-based coiled linear actuators (FCLAs) have been a significant research field in recent years, owing to their wide potential applications, such as artificial muscle^[1], intelligent robots^[2-3], prosthetic limbs for medical care^[4], deformable textile^[4] and energy harvesting^[5]. Comparing to traditional electromagnetic actuators and pneumatic actuators, this type of actuator is light, flexible, high contractile and versatile for multi-scale devices^[6]. The basic actuating principle lies in the anisotropic thermal/swelling and mechanical properties of the fiber, where the expansion/contraction in the radial direction is largely different from that in the axial direction during temperature change^[4], solvent-absorption/desorption^[7-8]etc.

FCLAs first reported were made from one-dimensional twisted assembly (yarn) of carbon nanotubes which was infiltrated by paraffin wax, or polyethylene glycol etc. The FCLA could be actuated by thermal, photothermal and chemical methods with high resistance to fatigue in cyclic tensile deformation^[1]. This guest-infiltrated FCLA achieved tensile actuation of -2.7% when heated from room temperature to 200 °C. Afterwards, more cost-effective FCLAs made from twisted polyamide monofilament (fishing line) and multi-filaments (sewing thread) were demonstrated with a larger tensile actuation of -49% at stress of 1 MPa when heated from 20 °C to 120 °C^[4]. However, most of the actuation happened at temperature higher than 60 °C, it is not suitable for human-related applications. An FCLA working at low temperature was reported based on low-density polyethylene monofilament, which had a tensile actuation of 10% at a higher stress of 20 MPa from 30 °C to 60 °C^[9]. The actuating strokes and stress were limited by the selected types of materials as their intrinsic properties can only satisfy certain requirements. For instance, the polyamide polyethylene fibers became brittle at low temperature thus their FCLAs are not suitable for such application scenarios.

A strain-programmable FCLA with bimorph polymer structure achieved tensile actuation of -11.8% with a very small temperature change from 20 °C to 30 °C [10]. The FCLA comprised of two components side-by-side: polyethylene and cyclic olefin copolymer elastomer. Cold drawing process resulted in plastic deformation of polyethylene while the other tended to recover to its original state, thus forming a tendril-like structure. The specification (spring diameter and spring index) and performance (tensile actuation and work density) could be programmed by adjusting the cold-drawing strain, speed and stress. Nevertheless, the actuation stress of this bimorph structured actuator is only 0.07 MPa, two or three orders of magnitude smaller than the coiled nylon monofilament FCLA (83.6 MPa) and 20% of stress of natural muscle (0.35 MPa). The volume fraction of each component was not adjusted for optimizing the performance.

The performance above mentioned actuators are limited by the materials used. The axial and radial expansion coefficients are determined by the fiber crystalline-amorphous structures. The size, amount and orientation of the discontinuous crystalline regions cannot be precisely designed and controlled during the fiber manufacturing process. If using the thermal energy, the actuators are heated/cooled by conduction from/to external source, leading to a low energy conversion efficiency and slow response. If using swelling mechanism for actuating, the diffusion processes will take some time thus the path length should be shortened for high response speed. The thermal and hygric wakening phenomena of these actuators are unavoidable. Their working environmental conditions are limited as the polyamide or polyethylene actuators cannot work at low temperature (say, -50 °C) because of their brittle failure.

This paper postulates that a new approach of engineered fiber composites as it offers great promises for solving the above mentioned problems as well as opens a door for a wide range of design options in terms of materials and device structures. Here we present such an approach for engineering design of programmable and thermally-

hardening helical composite yarn actuators (HCYAs) with a wide range of operating temperature by illustrating a working example.

We considered transition temperatures, thermal expansion coefficients and safety data of several fibers and matrix materials (Table S1), then selected polyimide (PI) fiber and polydimethylsiloxane (PDMS) to make composite yarn and further fabricate thermally powered **PI/PDMS** HCYAs (Figure 1A) because of their high temperature resistance, ductility under extremely cold condition, high anisotropic thermal expansion and biological safety. The volume fraction of each component was adjusted for desirable actuating performance. The resultant **PI/PDMS** HCYA could perform well under extremely low temperature from $-50\text{ }^{\circ}\text{C}$ to $100\text{ }^{\circ}\text{C}$ with an excellent linearity ($R^2=0.99927$). It offered a tensile actuation up to -16.8% at a stress of 1.2 MPa in isotonic test. An unusual temperature hardening effect was discovered, where the tensile stiffness of this **PI/PDMS** HCYA increased with the rise of temperature. This phenomenon is contradictory to most polymer materials whose moduli normally decline with an increasing temperature, attributing to atomic vibration, inter-atomic separation or rotational or vibrational movement of long-chain molecular polymer. The thermally-hardening effect was attributed by the coiled composite yarn structure, depicted by a thermomechanical model. Electrothermally powered HCYAs were designed, fabricated and tested by a **PI/Cu/PDMS** composite yarn. The performance of the thermally-driven **PI/PDMS** HCYAs and electrothermally-driven **PI/Cu/PDMS** HCYAs were presented and compared in terms of coil level, volume fraction of PDMS, actuating stress etc. Finally, two application prototypes with electrothermally powered **PI/Cu/PDMS** HCYAs were demonstrated as a tunable compression bandage and gripping hand robotics. This work creates new space of study to explore high performance and novel properties of actuators by appropriate composite structural design.

Results and discussions

Two types of HCYA are illustrated in Figure 1A. One dimensional (1D) composite with

multiple PI filaments and PDMS as the matrix. The other is a composite with copper coated PI filaments embedded in PDMS. The 1D composites were impregnated by PDMS/ethyl acetate solution then vulcanization in oven at 80 °C. The 1D composites were twisted under tension to form coiled HCYAs. A 1D composite undergoes two stages of buckling, which resulted in, at beginning, single coiled structure as shown in Figure 1H. As the twisting continues, a double coil structure appears upon the onset of the second buckling (Figure 1I), and finally the double coil structure overtakes the whole HCYA (Figure 1J). **As PDMS fully infiltrated into the space of hundreds of PI filaments (see figure S7), the integration between PDMS and PI yarn was rather intense, and no disintegration happens for PDMS.** The HCYAs were heat set at elevated temperatures.

Since the HCYA works based on anisotropic thermal and mechanical properties of the 1D composite or yarn, a large difference in the radial coefficient of thermal expansion (CTE) and the axial CTE is most desirable. As shown in Table S2, the PI filament has a negative axial CTE value, implying contraction in length when heated, while its radial CTE is smaller compared with PDMS thus ignored. PDMS is isotropic and has a large positive CTE, which facilitate the significant radial expansion of PI/PDMS composite yarn. Because of the large difference between axial CTE and radial CTE of composite yarn, the tensile actuation can be realized through composite structure. Besides, the 1D composite has a moderate axial modulus, according to the law of mixture, between that of PI filament and PDMS matrix, thus allowing sufficient actuation stress of **PI/PDMS** HCYA based on it.

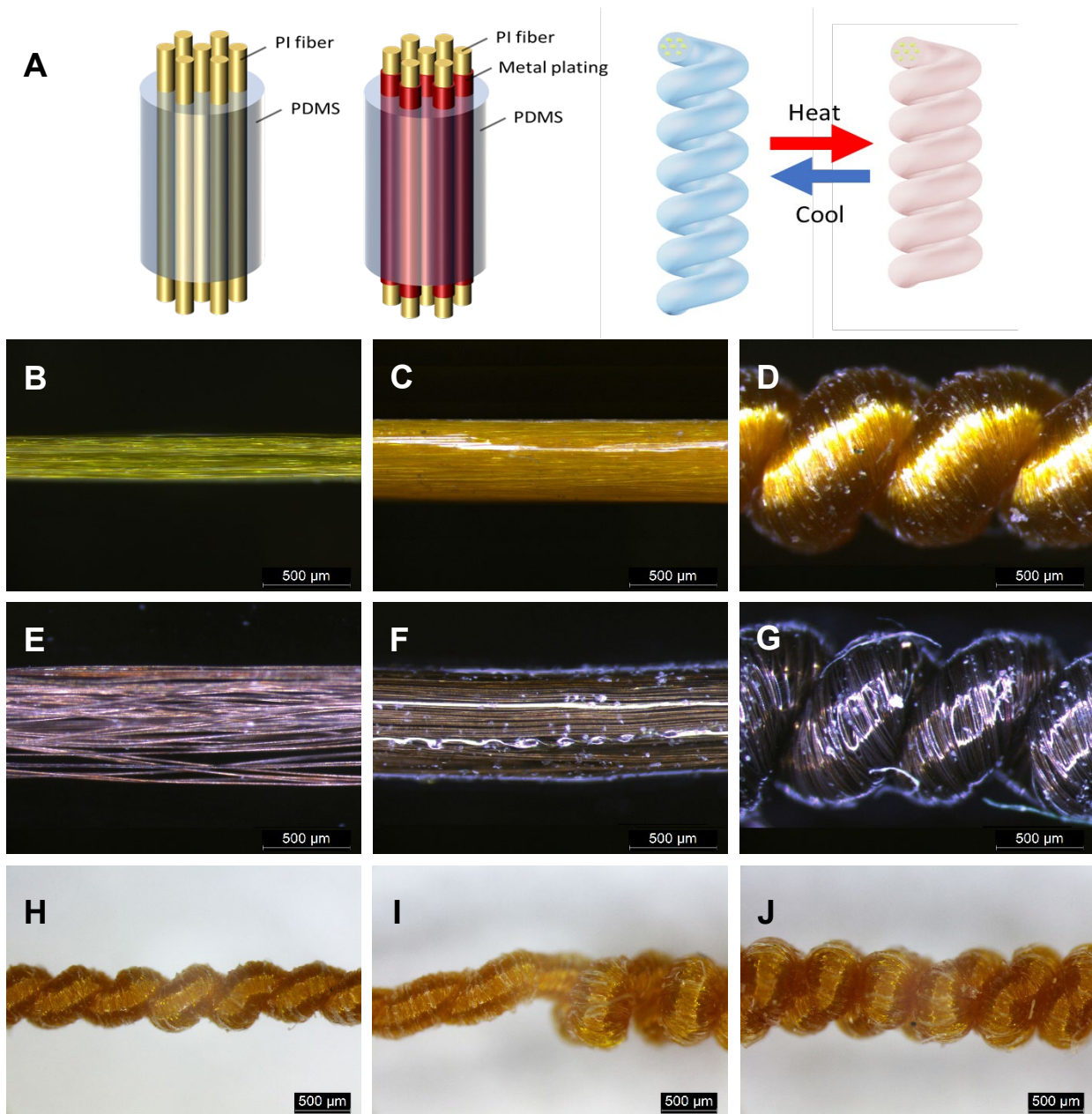


Figure 1 Composite yarns and thermally/electrothermally powered actuator. (A) Structure and components of composite yarn and spring-like thermally/electrothermally powered HCYA; (B) PI multifilament yarn (100 filaments); (C) PI/PDMS 1D composite (600 filaments); (D) PI/PDMS HCYA (600 filaments); (E) Cu coated PI yarn (100 filaments); (F) PI/Cu/PDMS composite (300 filaments); (G) PI/Cu/PDMS HCYA (300 filaments); (H) **PI/PDMS** HCYA with single-level coil; (I) **PI/PDMS** HCYA with single-double-mixed coil; (J) **PI/PDMS** HCYA with double-level coil.

Padding method was adopted for the PDMS impregnation process, as the evenness in dimensions was much better than those obtained by other methods (e.g. dip coating, glass board method, nozzle coating. Figure S4~S6). Volume fractions of constituent components are critical indices for composite design. Many influencing factors include the dimension and number of filaments, the concentration of PDMS/ethyl acetate solution, padding method, and number of repeated padding cycles. The volume fractions increase proportionately with the increasing percentage of PDMS in the coating solution for both dip-coating and padding method, i.e. the double of concentrations cause the approximate double of volume fractions. Padding method offers a little higher volume fraction than dip-coating method (Table S3). The volume fraction of PDMS can be readily controlled by the number of repeated padding cycles. A high volume fraction of 78.5% can be realized with padding four times. The volume fraction of PDMS increases with more filaments. An explanation is that increasing the number of filaments increases the amount of surface area for the absorption and retention of PDMS/ethyl acetate coating solution, thus resulting in more deposition of PDMS.

The morphology of multifilament yarn, 1D composites and resultant HCYAs are shown in Figure 1B~1G. The PI yarn, made of 100 filaments and a linear density of 200 Denier (grams per 9000 meters), was loose and even. Six such PI yarns were combined and PDMS was impregnated by dip-coating. After the vulcanization at 80 °C for 60~180 minutes, depending on the size of the sample, they formed a solid 1D composite with smooth, lustrous and even surface. The 1D composite was twisted and coiled into thermally powered **PI/PDMS** HCYA subsequently. Another processing route was to implement copper-plating of PI yarn before PDMS impregnation. Figure 1E shows that the plated yarn became much looser than the original yarn due to gas bubbles formed on fiber surface during the plating process. The looser packing facilitated a higher volume fraction of PDMS in the composite, see Figure 1F and Figure 1C. **For coating Cu-plated PI yarn with PDMS, the PDMS penetrated into the interspace of yarn, leaving part of copper on the surface of PI/Cu/PDMS composite yarn, which offered the**

conductivity. After twisting the PI/Cu/PDMS composite into coiled structure (Figure 1G), the electrothermally powered **PI/Cu/PDMS** HCYA had an electrical resistance of approximately 1 ohm/cm.

The morphologies of **PI/PDMS** HCYAs with three types of coil level (single-coil, single-double-mixed-coil, double-coil) are shown in Figure 1H~1J. The single-coil actuator possesses larger bias angle (i.e. the angle between radial direction of HCYA and tilted coil, see $\angle \alpha$ in Figure S12A) than the double-coil part. We found that single- and double-coiled HCYAs are much more steady in actuation strokes than the single-double-mixed-coil actuators, despite they have a potential to achieve higher actuation stroke, as the phase change from single-level to double-level coil can offer a more significant longitudinal change. Unless specified, the single-coil HCYAs are referred in this paper.

A heat-setting treatment close to or above the transition should be implemented to the twisted and buckled composite yarn by eliminating internal stress. Though treating at 380 °C can obtain stable actuators, many PDMS crack appeared on the surface, as shown in Table S4, which led to low performance in actuation stroke (Figure S9). **PI/PDMS** HCYA with 180 filaments achieved higher actuation stroke than that of **PI/PDMS** HCYA with 90 filaments, owing to higher volume fraction of PDMS resulting from more filling gap among filaments. Therefore, overheat-setting can reduce the actuating performance of thermally powered actuator, whereas low-temperature or even no heating setting may maintain the effective actuating ability. More PDMS content in the actuator facilitated better actuation stroke. **This conclusion is constant with the performances of 900f PI/PDMS HCYAs (Table S7).**

Thermomechanical properties of **PI/PDMS** HCYA was investigated in three modes, that is, isotonic (constant tensile load), isometric (constant tensile actuation) and isothermal mode (constant temperature). The results are presented as follows

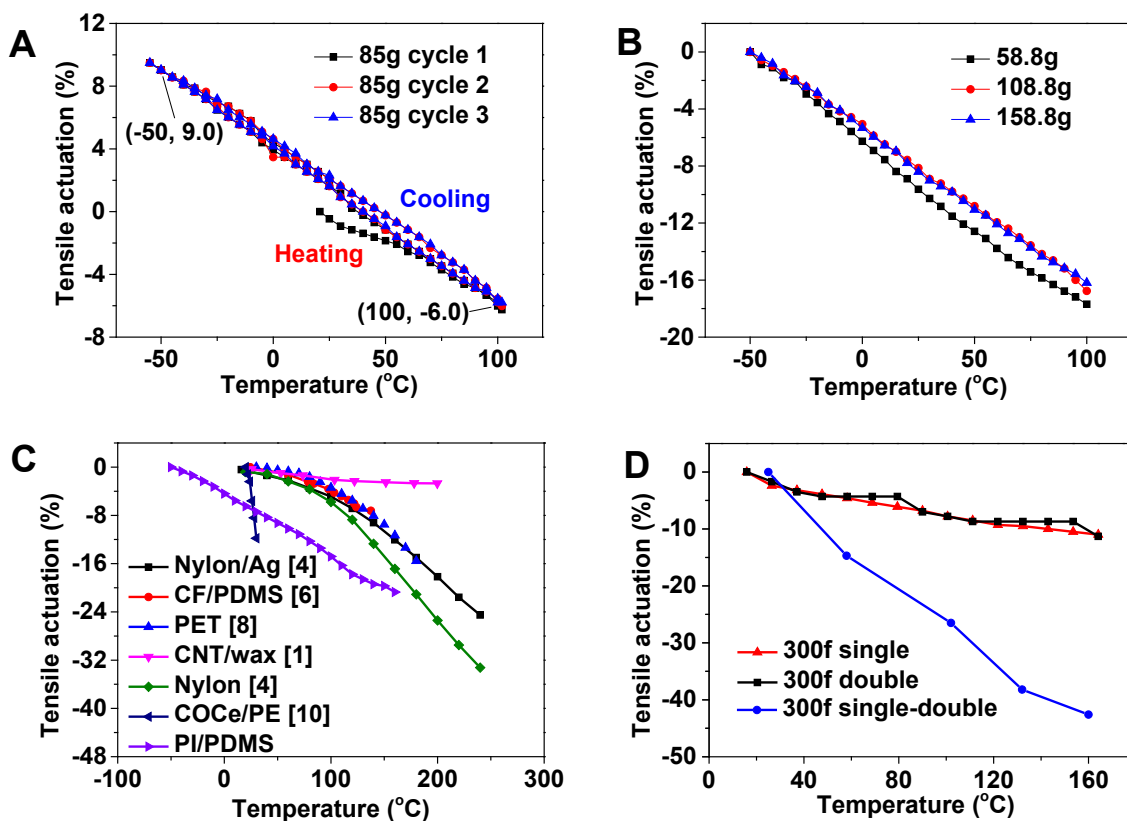


Figure 2 Isotonic results of HCYAs. (A) Isotonic performance of single-coil 600f PI/PDMS HCYA under 85g; (B) Isotonic test results of single-coil 900f PI/PDMS HCYAs under 58.8 g, 108.8 g, 158.8 g; (C) Comparison of isotonic behavior among various FCLAs, including nylon6,6/Ag FCLA with stress of >17 MPa^[4], Carbon Fiber/PDMS FCLA with stress of 60 MPa^[6], polyethylene terephthalate (PET) monofilament FCLA with stress of 6.2 MPa^[11], carbon nanotube (CNT)/wax FCLA with stress of 6.8 MPa^[1], nylon monofilament FCLA with stress of 83.6 MPa^[4], cyclic olefin copolymer elastomer/polyethylene (COCe/PE) FCLA with stress of 0.07 MPa^[10] and single-coil 600f PI/PDMS HCYA with stress of 1.2 MPa; (D) Tensile actuation of 300f thermally powered PI/PDMS HCYAs with single, single-double and double coil configurations.

Figure 2A illustrate the isotonic performance of single-coil 600f PI/PDMS HCYA under 85g. The “tensile actuation vs temperature” curves overlap each other in cycle 2 and

cycle 3, showing stable performance after the 1st cycle. The linearity of “tensile actuation vs temperature” curve was calculated as high as 0.99812 (calculated from -50 °C ~ 20 °C of cycle 2 and 20 °C ~ 100 °C of cycle 3). The isotonic test results of PI/PDMS HCYAs (9 yarns of 100 filaments each) under various load are shown in Figure 2B and Table S5. The tensile actuation of the PI/PDMS HCYA can reach up to -17.7% when the load is 58.8 g. As the load goes up, the tensile actuation slightly decreases, whereas both specific work and specific work capacity (defined as specific work divided by temperature change, i.e. 150°C) increase remarkably. The PI/PDMS HCYAs have specific works, ranging from 1.5 to 4.1 times higher than mammalian skeleton muscle.

Moreover, Figure 2C clearly demonstrates the highest tensile actuation of PI/PDMS HCYAs from 20 to 60 °C among all previously reported ones, that is, carbon fiber/PDMS, polyethylene terephthalate (PET) monofilament, carbon nanotube (CNT)/wax, nylon/Ag yarn and nylon filament. This actuation stroke results from the much higher thermal expansion of rubbery PDMS ($T_g = -123\text{ °C}$)^[12] than that of glassy PI fibers ($T_g > 60\text{ °C}$). Therefore, PI/PDMS HCYAs are more suitable for application under ambient condition, e.g. wearable and size-adjustable smart textiles.

Figure 1H~1J and Figure 2D show that the actuators can work well during a wide and high temperature range from 20 °C to 160 °C. Besides, the actuation curve of 300f single-coil actuator have better linearity, denoting a more stable performance than that of double coil and single-double-mixed coil. This can be attributed to the stable coil state. In this paper, we normally refer to the single coil actuators unless specified. Moreover, the single-double-mixed coil actuator can obviously achieve a high tensile actuation of -43.5%, which is caused by the coil state transition during the heating process. The large tensile actuation stemming from coil state change offers a new route to promote the deformation of actuators.

Tensile actuations and specific work capacities are summarized in Table S6~S7 for the

thermally powered **PI/PDMS** HCYAs of different filament number, coil level and volume fraction of PDMS. **600f** and **900f** HCYAs seem to reach higher tensile actuation owing to higher volume fraction of PDMS (Table S3). Double and single-double-mixed coil HCYAs can attain larger specific work capacity than that of single coil HCYAs, as remarkable tensile actuations came out during the coil state change from single to double when heated up.

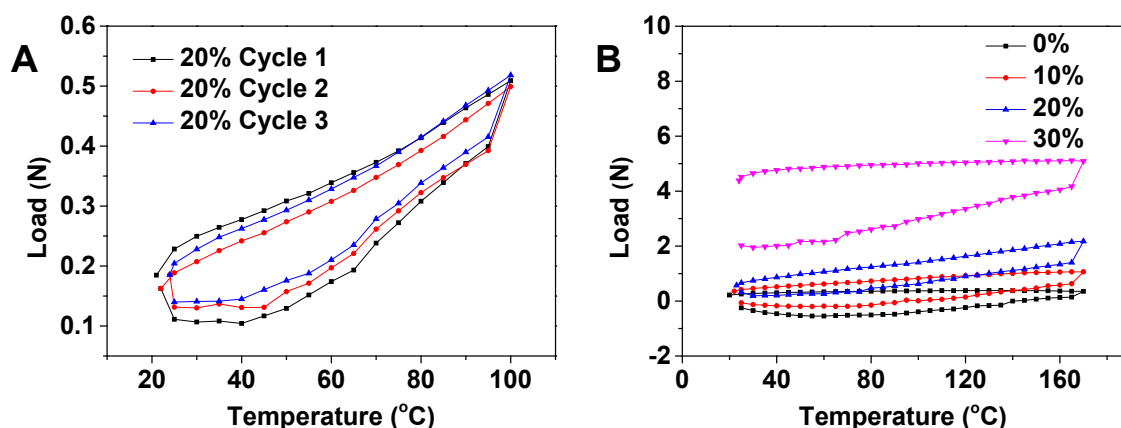


Figure 3 Isometric test results of 600f PI/PDMS HCYA. (A) Repeatability of PI/PDMS HCYA with a preset extension of 20% in three heating-cooling cycles; (B) PI/PDMS HCYA with various preset extension levels;

Isometric behaviors were investigated for 600f PI/PDMS HCYAs. For eliminating as much internal stress as possible, a higher heat-setting temperature (200 °C) was employed (effective working temperature is usually less than 180 °C). The 20% extended 600f PI/PDMS actuator became stable after the 1st cycle's heat-setting treatment at 200 °C as the curves of cycle 2 and cycle 3 are almost overlapped, as shown in Figure S10A. In subsequent isometric tests at 20 °C~100 °C (Figure 3A), the 20% pre-extended 600f PI/PDMS actuator shows good cyclability in 3 cycles, as well as that, the force nearly tripled from 0.18N to 0.51N (i.e. force increment is 0.33N), which is better than that of previously reported nylon monofilament HCYA (2.2 times load increase from 32 °C~123 °C)^[13]. This force enhancement can find its potential

applications in controllable compressive devices like stockings and garments with adjustable pressure.

Figure 3B reveals the effect of preset extension on the isometric behavior of 600f PI/PDMS HCYA. The slope of load-temperature curve from 20 °C to 170 °C is the highest when the extension is 20%, and the force increases nearly three times than that at 20 °C (from 0.57 N to 2.18 N). Both low and high preset extension don't facilitate the increase of force. Because a low preset extension of HCYA can restrain the effective actuation due to internal friction from close contact of adjacent coils, while a high preset extension directly leads to a large tension which could make the HCYA fatigue and lose efficacy.

After the heat-setting under extension rate of 20%, the sample curled up and became straight only when the extension was more than 17%. The sample was broken when the extension was over 36% during isotonic tests. Therefore, these two limit values were chosen for assessing the stability. The force enhancements were almost constant with time interval of approximately 100 hours for both samples, that is 0.26N for 17% extended sample and about 1.15N for 36% extended sample (Figure S10B and S10C), denoting that their force enhancement is stable over a long period of time.

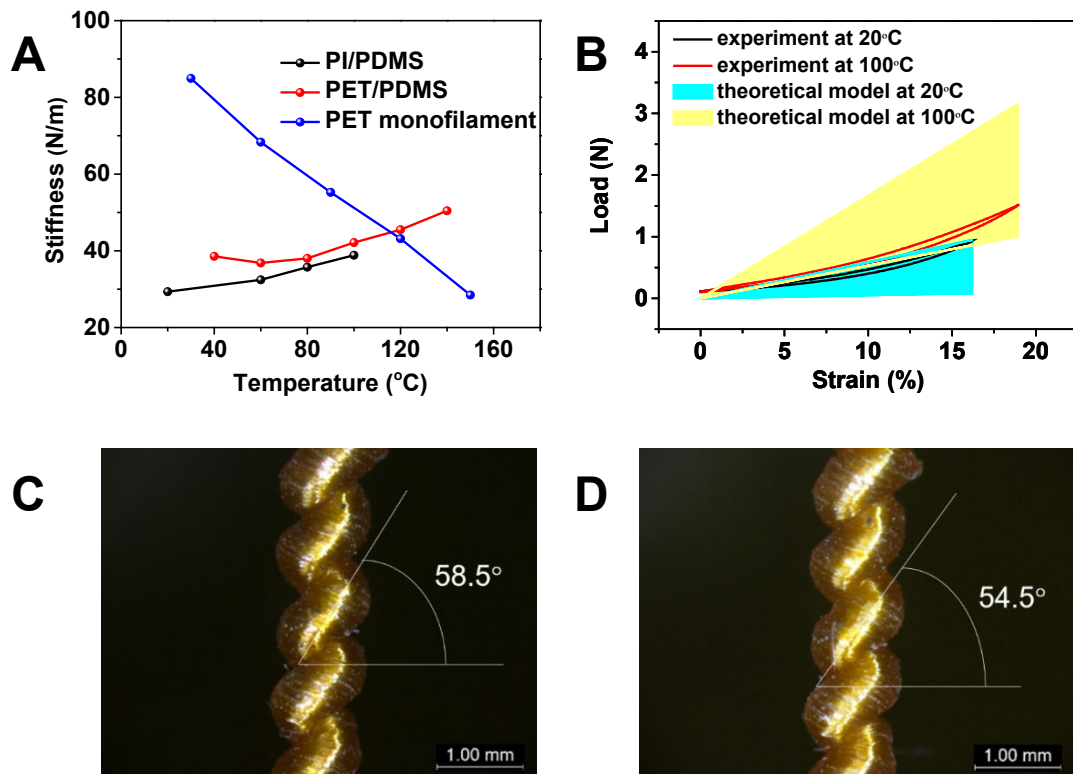


Figure 4 Stiffness changes of three different actuators with temperature and related theoretical analysis. (A) Stiffness vs temperature curves of actuators at strain of 15%; (B) Theoretical predictions of thermal-hardening HCYA at 20 °C (the blue area with upper and lower bounds estimates of measured α in the range of 57°~60°), and 100 °C (the yellow area with upper and lower bounds estimates of measured α in the range of 53°~56°) in isothermal tests; (C) Optic microscopy photos of 600f PI/PDMS at 20 °C in isometric test; (D) Optic microscopy photos of 600f PI/PDMS at 100 °C in isometric test.

Glass transition temperature (T_g) of yarn substrate and composite structure of actuator can affect the thermomechanical property of fiber-based coiled linear actuators, especially for the isothermal property. PET monofilament FCLA and PET/PDMS HCYA were selected to compare with PI/PDMS HCYA among a working temperature range of 20 °C ~ 150 °C, as the T_g of PET is 67 °C ~ 81 °C (within the range of working temperature), whereas that of PI is over 400 °C (much higher than the range of working temperature). Tensile properties of these three kinds of actuators under a

constant temperature are presented in [Figure S11A~S11C](#). As expected for most polymeric materials, as shown in Section 5 of Supplementary Materials, the tensile force and stiffness decrease with increasing temperature in the cases of the polyester monofilament ([Figure 4A and S11C](#)). [In the isothermal test for PI/PDMS HCYA, the length of sample was adjusted for ensuring the same initial load at different temperature.](#) The PI/PDMS HCYA, however, shows the surprising opposite ([Figure 4A and S11A](#)), that is, the force and stiffness increase with rising temperature, implying a phenomenon that the thermal-hardening instead of common thermal-softening of most polymer materials and structures. The multifilament PET/PDMS HCYA has a complex thermomechanical behavior, its tensile stiffness is first reduced from 40 °C until 60 °C then raised with rising temperature.

Experiments showed that the diameter of the three kinds of actuators increases when heating, which would remarkably change the geometrical configuration. Accordingly, the unusual isothermal behavior of PI/PDMS HCYA can be described, qualitatively as a structural effect, or a balance between two competing factors, that is, the diameter increase of spring-like anisotropic HCYA (promote modulus) and the molecular mobility change in the axial direction (reduce modulus) ([Figure S11D](#)).

In the cases of monofilament PET monofilament FCLAs ([Figure S11C](#)), though their spring-like structure and anisotropic property helped to offer extra contractive force/stiffness upon heating, the molecular mobility in the axial direction raised greatly as the actuating temperature were higher than their T_g , thus the contractive force/stiffness could be reduced by the relative slippage of molecular chains in the axial direction. Thus the tensile stiffness of PET monofilament FCLA went down with the rising temperature, as the reducing effect was larger than the promoting effect.

The multifilament PET/PDMS HCYA has more complicate isothermal behavior (Figure 4A). The stiffness of PET/PDMS HCYA goes down when heated from 40 °C to 60 °C (< T_g of PET) and increases when further heated from 80 °C to 180 °C (> T_g). It was because the reducing effect of molecular mobility was a little higher than the promoting effect of diameter increase when the heating temperature approached to T_g of PET. Nevertheless, the situation reversed when the temperature exceeded the T_g of PET, as the synergistic expansion of both PDMS and amorphous PET contributed to larger diameter increase which made the promoting effect dominated the tensile property. In the case of monofilament PET FCLAs, there is no, or very little of the structural anisotropic thermal expansion effect, thus the reducing effect takes the predominant role in the tensile properties.

When the PI/PDMS HCYA worked in a temperature range from -50 °C to 200 °C, the PDMS was in its rubbery state, PI was in a glassy state far below its glass transition temperature (T_g) (about 440 °C), the molecular mobility of the two phases hardly changed in the axial direction, thus the tensile modulus of PI/PDMS composite reduced at constant rates. Meanwhile the diameter increase of spring-like anisotropic composite yarn could remarkably raise contractive force^[4] and promote the stiffness during the rise of temperature, as the thermal expansion of the composite yarn in the radial direction far exceeded that in the axial direction.

To describe these two factors, i.e. molecular mobility in the axial direction and diameter increase of spring-like anisotropic composite yarn, a semi-quantitative thermo-mechanical model was explored for explaining this unusual thermal hardening effect of PI/PDMS HCYA. The mechanical behavior of PI/PDMS HCYA in tension is dependent on the material properties and geometrical configurations. The effective tensile modulus of PI/PDMS HCYA under longitudinal force is theoretically derived based on the assumption that materials behave linearly elastic, and anisotropic mechanics of

composites is adopted. Results show that the tensile modulus of **PI/PDMS** HCYA, K , is determined by the following function:

$$K(T) = \frac{\frac{[\sin 2(\alpha + \theta)]^2}{4} \left[1 - a_1 \left(\frac{T}{T_1^r} \right) \right] E_1^r A_1 + \left[1 - a_2 \left(\frac{T}{T_2^r} \right) \right] G_2^r A_2}{\sin^2 \alpha}$$

where α and θ are two angles of the geometrical configuration, respectively (Figure S12); a_1 and a_2 are material constants of PI and PDMS, respectively; E_1^r is the Young's modulus of PI at a reference temperature T_1^r ; G_2^r is the shear modulus of PDMS at a reference temperature T_2^r ; A_1 and A_2 are ratios of cross-sectional area of PI and PDMS in the composite yarn, respectively; T is the temperature variable. Derivation of the model is given in Section 6 of the Supplementary information. The calculation parameters are provided in its Section 7. **In linear elastic range, the overall load is proportional to the strain, where the proportion equals the product of tensile modulus and cross-sectional area. As the modulus $K(T)$ is derived as a function of temperature, and the cross-sectional area is directly measured, the slope of the theoretical load-strain curve varies with temperature.**

Substituting all the parameters into the theoretical model, the load-strain curves of **PI/PDMS** HCYA at 20 °C and 100 °C are plotted in **Figure 4B**, together with the experimental results. Due to the high sensitivity to the angle α measured on the photos, there is a large range of error, the shaded areas are the estimated ranges, with the upper and lower bounds determined accordingly, as shown in **Figure 4B**. The predicted influence of temperature is in a reasonable agreement with the experiments. The theoretical model investigates the mechanism of thermal hardening in the actuation of **PI/PDMS** HCYA, and semi-quantitatively predicts the variation of mechanical behavior with temperature. It provides guidelines to adjust the parameters. In particular, the orientation angles among the fibers, yarns and HCYA are found to be predominant, which needs further optimization in future work. The unusual thermal-hardening property can be achieved by optimizing the composite coiled structure, using appropriate parameters, in particular the predominant orientation angles among the

fibers, yarns and HCYA. This unusual thermomechanical property has potential applications in the field where needs arise for high stiffness under high temperature, e.g. heat-resisting materials.

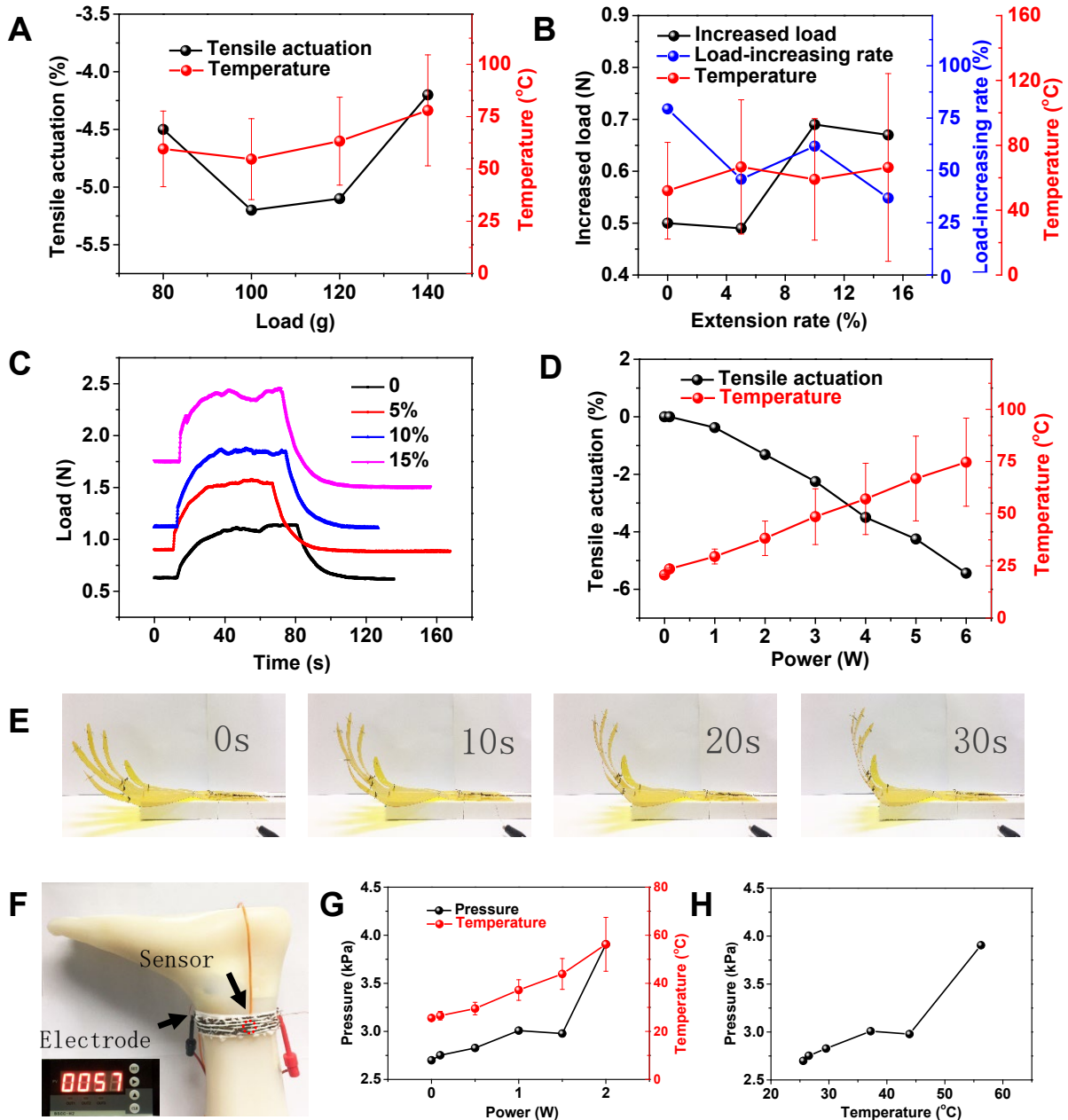


Figure 5 Electro-thermo-mechanical actuation and applications of 2-ply 300f PI/Cu/PDMS HCYA. (A) Tensile actuation and temperature of PI/Cu/PDMS HCYA with different tensile loads in isotonic tests with an input electric power of 1.5W; (B) Effect of pre-extension on changes of tensile force in isometric tests with an input

electric power of 1.5W; (C) Tensile-force-time curves of **PI/Cu/PDMS** HCYA with various pre-extension; (D) Tensile actuation and working temperature plotted against input electric power in the isotonic tests for actuating fabric; (E) Robotic hand actuated by **PI/Cu/PDMS** HCYAs; (F) Pressure measurement set-up of the pressure-adjustable compression bandage on a lab-made smart leg manikin ^[14-15] by piezoresistive sensor (red round dash line); (G) Measured pressure and temperature plotted against input electric power; (H) Pressure as a function of temperature.

In order to conveniently heat and control HCYAs, electro-thermally powered **PI/Cu/PDMS** HCYAs were fabricated from copper-plated PI fibers and PDMS (Figure S13A). Two **PI/Cu/PDMS** composite yarns were plied for improving continuous conductivity, followed by super-twisting into **PI/Cu/PDMS** HCYA. Then, the **PI/Cu/PDMS** HCYA was joule-heated by electricity (input power of 1.5 W) in isotonic tests. Figure 5A shows that the tensile actuation stroke of **PI/Cu/PDMS** HCYA increases from 4.5% to 5.2% when the actuating load raises from 80 g to 100 g, then drops down with heavier actuating load. This case is consistent with that thermally driven **PI/PDMS** HCYA (Figure 2A~2C) due to the same reason of balance between touch of the adjacent coils and fatigue of the HCYA. Under the optimal load of 100 g, the maximum working temperature is about 60 °C, making the **PI/Cu/PDMS** HCYA suitable for wearable functional devices, e.g. exoskeleton muscles, compression garments etc. **As the plated copper layer is not even on the PI yarn substrate, the temperature is not even along the HCYA. Therefore, the error of temperature was evaluated by standard deviation of three temperature values recorded by IR camera, including maximum value, minimum value and medium value.**

Besides, the actuation performance of **PI/Cu/PDMS** HCYAs made from different numbers of PI fibers is presented in Table S8. The **PI/Cu/PDMS** HCYA of 600 PI filaments has a higher tensile actuation of 17.9% with an input power of 1.9 W, a low

voltage of 5.95 V (movie S1), and a higher temperature of 162 °C, thus may be applied effectively in robotic or industrial use. On the contrast, the **PI/Cu/PDMS** HCYA with 300 PI filaments has less actuation stroke of 4.2 % with input power of 0.6 W, voltage of 3.87 V, and temperature of 63 °C, suitable for wearable applications. The obvious disadvantage is their long actuation time of about 30s, which leads to a low energy conversion efficiency. This may be caused by the low thermal conductivity of PDMS ($0.15\sim 0.2 \text{ Wm}^{-1}\text{K}^{-1}$)^[12], which impedes the prompt heat conduction from the conductive copper layer to the whole **PI/Cu/PDMS** HCYAs.

Afterwards, isometric tests of the **PI/Cu/PDMS** HCYA with different pre-extension were implemented and the heating was done by electric power of 1.5W (Figure 5B and Figure S13B). The load increment is low and load increasing rate is high when the pre-extension is 0, whereas the load increment becomes high and load increasing rate becomes low when the pre-extension reaches 15%. The optimal pre-extension is 10%, with which a high load increment from 1.12 N to 1.81 N and load increasing rate of 61.6% can be obtained simultaneously. Low pre-extension leads to mutual squeezes of adjacent coils and the consequent low load increment, whereas the low initial pre-extension (denominator during calculation) contributes to the high load increasing rate.

The load peaks within 20 seconds if heating with 1.5 W and goes back to the initial load within about 20s after switching off the power for pre-extension of 5%, 10% and 15% (Figure 5C). It takes longer time for the **PI/Cu/PDMS** HCYA with zero pre-extension to peak due to compact coils. The significant load enhancement and satisfactory response time facilitate its applications where controllable changes in tensile force or pressure are desirable, e.g. message compressive stockings or pressure controllable bandages.

To demonstrate their applications, a robotic arm was constructed by 3D printing using polylactic acid. Figure 5E shows that elastomeric yarns attached to the fingers were

used for taking the fingers back, while **PI/Cu/PDMS HCYA** were used to offer contractive force for the grabbing action of the robotic hand. A tensile actuation of -2.9% was obtained with electric power of 4.8W (Figure 5E and movie S2). Moreover, the robotic arm can also be actuated in an extremely cold environment of -50 °C, achieving the same actuation with doubled input electric power (movie S3).

Another demonstration was a pressure adjustable bandage woven by a handloom machine. **The PI/Cu/PDMS HCYAs were employed as the weft yarn for driving effect and polyester multifilament textured yarns as the warp for keeping the integration of bandage (sateen woven in Figure S13C).** The polyester textured yarns and the PI/Cu/PDMS HCYAs were intertwined alternatively for ensuring effective contraction. Conductive wires were twined at the two ends of the fabric as connection electrodes. A DC power source was employed to heat the actuating fabric, which was loaded with 600 g (Figure S13D). Both temperature and tensile actuation increase with the rise of input electric power. A tensile actuation of about 5.4% was achieved as the temperature reached 75 °C approximately in isotonic test (Figure 5D). The tensile force increment of the bandage can be used to tune the pressure level exerted on human body in isometric configuration. Figure 5F shows the experimental set-up for the pressure measurement on a lab-made soft smart leg mannequin with optical grating sensing network and a piezoresistive sensor (has been calibrated to remove temperature effect, Table S10). The measured pressure and temperature increase, in general, with increasing input electric power (Figure 5G and 5H). The pressure increases from 2.699 kPa to 3.905 kPa, when the temperature rises from 25.6 °C to 56.2 °C, achieving a pressure change of 1.206 kPa and relative pressure increment of 44.7%. **A pressure drop happens when the power is 1.5W, as the surface of actuating fabric and HCYA is not absolutely even (Figure 1G). If the coils expand and move horizontally when joule-heating, the pressure will change accordingly.** The pressure adjustable bandage may find its future wearable applications in the treatment of burn patients, adjunctive therapy of varicose vein and other compression garments^[16-17].

Conclusions

In order to achieve high actuation performance and novel properties, as well as working at extreme conditions, we have overcome the great difficulties of current limited selection range of materials by engineered one-dimensional composites with a wider selection range of constituent materials and adjustable structure. PI/PDMS thermally powered HCYAs were taken as an example and fabricated by pad-coating and super-twisting process. After characterization in isotonic, isometric and isothermal modes, In isotonic mode, the fabricated **PI/PDMS** HCYAs achieved high tensile actuation (-20.7%) under relatively heavy load of 1.2 MPa within wide temperature range (-50~160 °C), excellent linearity ($R^2=0.999$), competitive specific work (158.9 J/kg, 4 times of natural muscle) and low hysteresis (6.7%). The isotonic behavior of **PI/PDMS** HCYAs was optimized by appropriate volume fraction of matrix, filament number and coil level. Besides, the **PI/PDMS** HCYAs showed high reactive force, load enhancing rate (nearly tripled), as well as good stability and cyclability in isometric mode, denoting their potential application in pressure-tunable compressive devices. Most importantly, unusual thermally hardening phenomenon was found in these **PI/PDMS** HCYAs, illustrating the heat resistance and thermal-hardening effect can be realized simultaneously in a composite structure through appropriate composite structural design. A thermomechanical model of **PI/PDMS** HCYA was established to provide the upper and lower bounds of this effect on effective modulus of **PI/PDMS** HCYAs with a reasonably good agreement of experimental results.

In addition to thermally driven **PI/PDMS** HCYAs, electrically conductive copper layer was coated on the PI filaments before the composite fabrication. The resultant **PI/Cu/PDMS** HCYAs was powered electrically and maintained their actuation performances in isotonic and isometric modes. Prototypes of pressure-tunable compressive bandage and robotic hand were demonstrated for their potential applications in robots and wearable compression devices.

The present work starts a new route to engineering design fiber-based actuator materials and structures for high performance, novel properties, and working at extreme conditions.

Experimental section

Fabrication of composite yarns and actuators: Polyimide (PI) filament yarn of 200D/100f (Suplon®, Aoshen, China), as well as polyester (PET) filament yarn of 150D (Dhoma, China), was used as host material of the composite yarn. **200D/100f means the yarn has a fineness of 200 Denier and 100 filaments.** Polydimethylsiloxane (PDMS) liquid silicone rubber (ELASTOSIL® LR 7665 AB, Wacker, Germany) was selected as polymer matrix to offer an expansion in radial direction of the PI/PDMS composite yarn. Ethyl acetate (ACS Grade, ANAQUA, Hong Kong) was adopted to dilute PDMS for lowering down the viscosity and coating the PI filament yarn evenly.

For fabricating PI/Cu/PDMS composite yarn, PI yarn was firstly copper-plated by two groups of solutions (A: NaOH, 12g/L; CuSO₄·5H₂O, 13g/L; KNaC₄H₄O₆·4H₂O, 29g/L. B: HCHO 9.5mL/L.) after a series of pretreatments, including hydrophilic treatment (2.5mol/L KOH solution), sensitization (11.9 g/L SnCl₂·2H₂O and 40mL/L 37% HCl) and activation (0.25g/L PdCl₂ and 40mL/L 37% HCl). Then the two ends of copper-plated PI yarn were protected by two layers of PI film (thickness: 0.05mm) which were stuck together through 3M VHB Tape 4905 for avoiding the reduction of conductivity. Finally, PDMS coating was carried out by padding method as follows.

PI yarns (with filament number of 90, 180, 270, 300, 600 or 900), PET yarn or PI/Cu yarns were dipped into PDMS/ethyl acetate solution (w:w=1:2), followed by getting through a padder with two rollers (Figure S1). An appropriate distance of gap between the two rollers was set for controlling the uptake of PDMS/Ethyl acetate solution. A digital level was set on a cantilever, which connected with upper roller through a vertical steel pillar. When adjusting the cantilever to certain angle recorded by digital level, the upper roller can change its height, thus the distance of gap changes accordingly. The level angle

of cantilever is $-1.3^{\circ} \sim -1.7^{\circ}$, rolling speed of roller is 7 round per minute.

After dipping and padding once or several times for achieving high volume fraction of PDMS (Table S3), the PDMS-coated PI yarns, PET yarns or PI/Cu yarns were vulcanized at 80°C for 3h prior to the composite yarns were achieved, e.g. 300f PI/PDMS composite yarn, 600f PI/PDMS composite yarn, 900f PI/PDMS composite yarn, PET/PDMS composite yarn, PI/Cu/PDMS composite yarn etc.

Thermally powered actuators were fabricated by an experimental setup as Figure S2. The two ends of PI/PDMS composite yarns were nipped by small drill chucks, then one end of the nipped composite yarn was fixed into the hole of stirring head of stirrer (IKA RW 20) while another end was stretched by a proper load (Table S9) and prevented from rolling by a metal pin. Magnetic induced counter (GQGH, HB961, China) was used to test the twisting number by sensing the movement of a magnet stuck on the stirring head. The composite yarns were twisted until forming single-level coil state, single-double-mixed-level coil or double-level coil state (Figure 1H~1J). Single-double-mixed-level coil can be achieved though further twisting single-level coil actuator, while double-level coil actuator was completed after further twisting single-double-mixed-level coil actuator until all the coils formed the double-level coil state.

Characterization of composite yarns and actuators: For morphology, electron microscope (Leica M165 C or DFC290 HD) and scanning electron microscope (Hitachi TM3000) were deployed to measure the surface morphology, diameter, cross section, spring index and bias angles of composite yarn or HCYA.

Coefficient of thermal expansion of PI fiber or PI/PDMS composite yarn was determined by TMA (METTLER TOLEDO, TMA/SDTA 1+) in tension/compression mode for axial/radial direction and modulus of PI/PDMS composite yarn was tested by DMA (METTLER TOLEDO, DMA 1) through the same mode as above.

Thermomechanical properties of thermally powered actuators were assessed in terms of isotonic, isometric and isothermal test, wherein load frame (Instron 5566) equipped with a heating oven was used to carry out isotonic, isometric and isothermal tests at the temperature ranging from 20 °C to 200 °C, whereas climate chamber was applied to implement isotonic tests from -50 °C~100 °C. The real-time data of temperature and displacement were collected by temperature sensor (Asmik, MIK-ST500, China) and displacement sensor (Wen sheng wuxi, MYDJ-O, China), respectively. (Figure S3)

Weaving of fabric based on electrothermally powered PI/Cu/PDMS HCYA: Actuating fabric was fabricated on a manual weaving machine, applying the PI/Cu/PDMS HCYA as weft and cotton yarn as warp (texture: 3 up 1 down). Two groups of wefts made by spandex were woven as the edges beside the PI/Cu/PDMS HCYA for protecting them from falling off. Iron wires were twined on the two ends of the fabric as electrodes.

Fabrication of robotic arm with artificial muscle made by PI/Cu/PDMS HCYA: The robotic arm was 3D printed by Polylactic acid (PLA) plastic with Makerbot Replicator 5th Gen 3D Printer. Spandex was used for stretching fingers back, while nylon monofilaments connected with PI/Cu/PDMS FCLA were used to offer tensile force for grabbing of the robotic hand.

Acknowledgement

Z. Zhang and B. Zhu contributed equally to this work. The research has been funded by the Hong Kong Polytechnic University (Grant No. 480A) and a postgraduate scholarship for ZH Zhang from the same source.

References

[1] M. D. Lima, N. Li, M. Jung de Andrade, S. Fang, J. Oh, G. M. Spinks, M. E. Kozlov, C. S. Haines, D. Suh, J. Foroughi, S. J. Kim, Y. Chen, T. Ware, M. K. Shin, L. D. Machado, A. F. Fonseca, J. D. Madden, W. E. Voit, D. S. Galvao, R. H. Baughman, *Science* **2012**, 338

(6109), 928-32.

- [2] L. Wu, M. J. de Andrade, T. Brahme, Y. Tadesse, R. H. Baughman, *Proc. SPIE*, **2016**, p 97993K.
- [3] M. C. Yip, G. Niemeyer, *Proc. 2015 IEEE Int. Conf. Robotics and Automation (ICRA)*, IEEE, Washington State Convention Center, **2015**, pp 2313-2318.
- [4] C. S. Haines, M. D. Lima, N. Li, G. M. Spinks, J. Foroughi, J. D. W. Madden, S. H. Kim, S. Fang, M. J. d. Andrade, F. Göktepe, Ö. Göktepe, S. M. Mirvakili, S. Naficy, X. Lepró, J. Oh, M. E. Kozlov, S. J. Kim, X. Xu, B. J. Swedlove, G. G. Wallace, R. H. Baughman, *Science* **2014**, *343* (6173), 868-872.
- [5] S. H. Kim, C. S. Haines, N. Li, K. J. Kim, T. J. Mun, C. Choi, J. Di, Y. J. Oh, J. P. Oviedo, J. Bykova, S. Fang, N. Jiang, Z. Liu, R. Wang, P. Kumar, R. Qiao, S. Priya, K. Cho, M. Kim, M. S. Lucas, L. F. Drummy, B. Maruyama, D. Y. Lee, X. Lepró, E. Gao, D. Albarq, R. Ovalle-Robles, S. J. Kim, R. H. Baughman, *Science* **2017**, *357* (6353), 773-778.
- [6] C. Lamuta, S. Messelot, S. Tawfick, *Smart Mater. Struct.* **2018**, *27* (5), 055018.
- [7] P. Chen, Y. Xu, S. He, X. Sun, S. Pan, J. Deng, D. Chen, H. Peng, *Nat. Nanotechnol.* **2015**, *10* (12), 1077.
- [8] M. D. Lima, M. W. Hussain, G. M. Spinks, S. Naficy, D. Hagenasr, J. S. Bykova, D. Tolly, R. H. Baughman, *Small* **2015**, *11* (26), 3113-3118.
- [9] M. Hiraoka, K. Nakamura, H. Arase, K. Asai, Y. Kaneko, S. W. John, K. Tagashira, A. Omote, *Sci. Rep.* **2016**, *6*, 36358.
- [10] M. Kanik, S. Orguc, G. Varnavides, J. Kim, T. Benavides, D. Gonzalez, T. Akintilo, C. C. Tasan, A. P. Chandrakasan, Y. Fink, A. Polina, *Science* **2019**, *365* (6449), 145-150.
- [11] Z. Peng. Study on thermally activated coiled linear actuators made from polymer fibers. The Hong Kong Polytechnic University, Hong Kong, 2018.
- [12] A. C. Kuo, *Polymer data handbook* **1999**, 411-435.
- [13] A. Cherubini, G. Moretti, R. Vertechy, M. Fontana, *AIP Adv.* **2015**, *5* (6), 067158.
- [14] B. Yang, X. Wang, Y. Xiong, S. Liu, S. Liu, X. Tao, *Smart Mater. Struct. in press*.
- [15] B. Yang, S. Liu, X. Wang, R. Yin, Y. Xiong, X. Tao, *Sensors* **2019**, *19* (8), 1811.
- [16] Y. Xiong, X. Tao, *Polymers* **2018**, *10* (6), 663.

[17]J. Shi,S. Liu,L. Zhang,B. Yang,L. Shu,Y. Yang,M. Ren,Y. Wang,J. Chen,W. Chen,
Adv. Mater. **2019**.

Programmable and thermally-hardening composite yarn actuator with a wide range of operating temperature

Ziheng Zhang, Bo Zhu, Zehua Peng, Rong Yin, Ray H. Baughman*, Xiaoming Tao*

Supplementary Information

Section 1. Composite yarn fabrication by impregnation

1.1 Dip-coating method

PI yarn segments mentioned above were soaked into PDMS/ethyl acetate solution for a period (3 min~3 h), then elevated gradually with a speed of about 15 cm/min for obtaining even coating (Figure S4). Afterwards, the coated PI yarn segments were vulcanized by the same parameter as above prior to complete the fabrication of PI/PDMS composite yarn.

1.2 Glass board method

Glass board method is an impregnation process completed on a glass board rather than in the glass jar mentioned above. This method can achieve a high PDMS volume fraction of over 80%. The concrete steps are as follows:

- a. Cut 30cm long segment of the PI yarn, then draw out the monofilaments.
- b. Wind the monofilaments to metal framework, which two ends were winded by the double-sided tape (Figure S5A).
- c. Coat the fixed monofilaments with PDMS/ethyl acetate solution (1:2) on the glass board, then vulcanize PDMS at 150 °C for 30min. Repeat this step for 2 times (Figure S5B).
- d. Combine seven coated monofilaments into a yarn, which was then dipped into PDMS/ethyl acetate solution (1:5) without tension and vulcanized at 90 °C for one night (Figure S5C).
- e. Cool down in ambient air.

1.3 Nozzle-coating method

Nozzle-coating method means coating a monofilament by drawing it through a narrow nozzle and can achieve a high PDMS volume fraction. However, intermittent bead may form due to high surface tension between PI and PDMS. (Figure S6) The steps were as follows:

- a. Get syringe half-filled with PDMS.
- b. Insert an iron wire (200 μ) which is wound by PI monofilament.
- c. Fix a nozzle (400 μ) on the head of syringe.
- d. Draw iron wire out of nozzle for coating PI monofilament

Section 2. Distribution of PI fibers in PDMS matrix

Figure S7 show the cross-sectional views of the composite yarns.

Section 3. Twisting curve

The composite yarns of **300f**, **600f** and **900f**, were twisted under tensile loads of 60 g, 120 g and 180 g, respectively. The longitudinal change was measured as the twist number increased (Figure S9). The shortening speeds of twisted composite yarns become faster when single-level coils appear and even faster when double-level coils appear. The composite yarn with more filament number needs more twist number to form fully single-level or double-level coil state.

Section 4. Forming condition of single-level & double-level coils

Referring to twist composite yarn into single-level or double-level coil thermally powered actuator, weak stretching force may not achieve effective and stable coil state, whereas too strong stretching force may break the yarn. Therefore, selecting proper loads for twisting the yarns is very important for fabricating actuators. The forming conditions of single-level and double-level coils are shown in Table S9. A tensile force of 8.7 g is enough to form single-level coils for all the types of yarns, i.e. **300f** uncoated, **300f** coated, **600f** coated and **900f** coated yarn, while these yarns do not break under the load of 108.7 g. However, forming double-level coil need heavier load for **600f** and

900f composite yarn, as light load cannot keep the linear state, only leading to randomly twine by the yarn itself. Considering a fact that lighter stretching load facilitate fabricating actuators of low bias angle, denoted by \underline{Y} , which may have higher potential to obtain larger tensile actuation, the suitable load for such composite yarn in Table S9.

Section 5. Temperature-modulus relationship of common polymer materials

The relationship between modulus and temperature can be depicted by the following formula:

$$\frac{E}{E_0} = [1 - a \left(\frac{T}{T_m} \right)]$$

where E represents the modulus of the material at temperature T and E_0 is modulus at 0K. T_m and a represent melting temperature and proportional constant of specialized crystalline material (most is 0.5), respectively^[1]. Therefore, the modulus should decrease with growing temperature. Figure 4C and 4D shows an isothermal behavior of PET monofilament FCLA in accordance with this common rule. The slope of load-strain curve, as well as tensile modulus, goes down gradually with increasing temperature from 30 °C to 150 °C. This result is constant with a nylon monofilament FCLA which tensile modulus (i.e. slope of stress-strain curve) kept dropping when the temperature ascended from 25 °C to 122 °C^[2].

Section 6. Derivation of the modulus-temperature relationship of single-coiled PI/PDMS HCYAs

Single-coiled HCYA has a spring-like 3D helix geometry (Figure S12A). Experiments showed that in heating, both α and β decrease and the longitudinal length of HCYA reduces in isotonic test, while α and β increase when HCYA is elongated in tension as sketched in Figure S12B; on the other hand, the curvilinear length of composite yarn and PI fiber almost keep unchanged. This phenomenon indicates that the actuation of HCYA is generated by the shear deformation of the yarn. In the elastic theory, the tensile stiffness of a conventional spring is determined from the torsion of the material along

the helix wire^[3]:

$$k = \frac{Gd^4}{8ND^3}$$

However, it is noted that the formula above is derived based on two assumptions. First, the spring is hollow inside, i.e. the diameter of spring, D , is much greater than that of wire, d . Second, the orientation angle α is very small close to zero. As for the present sample, the dimension of HCYA is comparable to the composite yarn, and α is significant, hence the conventional conclusion is not applicable. Considering that the HCYA is relatively dense with very little gap or void inside, an equivalent model of shear of the yarn is adopted, and the contribution of bending of yarn is estimated.

The configuration of yarn is simplified as a parallelogram element (Figure S12C). When a longitudinal tensile force P is applied, the shear stress on the element is

$$\tau = \frac{P \tan \alpha}{A/\sin \alpha} \quad (1)$$

where A is the cross-sectional area of yarn. Accordingly, the shear deformation of element results in length change Δ along the axis of HCYA.

$$\Delta = l\gamma \sin \alpha \cos \alpha \quad (2)$$

where γ is the shear strain induced, and l is the initial longitudinal length of element.

According to Hooke's Law, tensile strain in the longitudinal direction of HCYA is

$$\varepsilon = \frac{\Delta}{l} = \gamma \sin \alpha \cos \alpha = \frac{\tau}{G} \sin \alpha \cos \alpha \quad (3)$$

where G is the nominal shear modulus of the yarn. Combining (1) - (3), the tensile modulus of HCYA, K , is expressed as

$$K = \frac{\sigma}{\varepsilon} = \frac{\frac{P}{A/\sin \alpha}}{\frac{\tau}{G} \sin \alpha \cos \alpha} = \frac{G}{(\sin \alpha)^2} \quad (4)$$

Result shows that K depends on the nominal shear modulus of the composite yarn, as well as the angle α in the helix configuration.

Further consider the square element of composite materials of yarn, PI fibers are orientated along angle β to the longitudinal axis, filled with PDMS as matrix (Figure S12D). Due to anisotropy, the shear deformation of the composite is generated by both normal and shear stresses, which involves with the tension of PI fibers and the shear of PDMS matrix. By geometry, the tensile strain of PI fiber is

$$\varepsilon = \frac{\delta}{\frac{l}{\sin \beta}} = \frac{\frac{l\gamma \sin \beta}{\tan \beta}}{\frac{l}{\sin \beta}} = \gamma \sin \beta \cos \beta \quad (5)$$

From energy point of view, the work associated with the shear of yarn is transformed to the tensile energy of PI fibers and the shear energy of PDMS matrix.

$$W = \frac{1}{2}G\gamma^2V = \frac{1}{2}E_1\varepsilon_1^2V_1 + \frac{1}{2}G_2\gamma^2V_2 \quad (6)$$

where the subscript 1 represents PI, 2 represents PDMS, V is the total volume of composite yarn, E_1 and G_2 are Young's Modulus and Shear Modulus of PI fiber and PDMS matrix. As the volume ratio of PI and PDMS, V_1 and V_2 , equal the ratios of cross-sectional area, A_1 and A_2 , the nominal shear modulus of composite yarn is

$$G = (\sin \beta \cos \beta)^2 E_1 A_1 + G_2 A_2 \quad (7)$$

Note that the difference between α and β represents the angle of PI fibers, θ , relative to the transverse direction of yarn, which is approximately constant during actuation process, so β can be rewritten as

$$\beta = \alpha + \theta \quad (8)$$

Substituting (7) and (8) into (4), the tensile modulus of HCYA becomes

$$K = \frac{[\sin 2(\alpha+\theta)]^2}{4} \frac{E_1 A_1 + G_2 A_2}{\sin^2 \alpha} \quad (9)$$

The model describes the relationship between the modulus of HCYA and geometrical configuration, material properties, as well as composite constituents. During the

actuation, HCYA is first heated and the temperature change has effect on material modulus. As a simplified estimation for most crystalline materials, there is a linear relationship between modulus E and temperature T .

$$\frac{E}{E^r} = 1 - a \left(\frac{T}{T^r} \right) \quad (10)$$

where E^r is the modulus at a reference temperature T^r , and a is a coefficient depending on material. Combining (9) and (10), the tensile modulus of HCYA is expressed as

$$K = \frac{\frac{[\sin 2(\alpha+\theta)]^2}{4} \left[1 - a_1 \left(\frac{T}{T_1^r} \right) \right] E_1^r A_1 + \left[1 - a_2 \left(\frac{T}{T_2^r} \right) \right] G_2^r A_2}{\sin^2 \alpha} \quad (11)$$

To evaluate the bending effect of yarn, the radius of curvature of the yarn segment in 3D space as illustrated in Figure S12E is

$$\rho = \frac{h}{\pi \sin \alpha} \quad (12)$$

where h is the height of the yarn segment along the axis of HCYA. When HCYA is elongated, the radius of curvature increases to

$$\rho + \Delta\rho = \frac{h + \Delta}{\pi \sin(\alpha + \gamma \sin^2 \alpha)} \quad (13)$$

According to the bending theory,

$$\frac{M}{EI} = \frac{1}{\rho} - \frac{1}{\rho + \Delta\rho} \quad (14)$$

where M is the effective bending moment, E is the effective Young's Modulus of yarn, and I is the effective moment of inertia for bending. Combining (12), (13) and (14), and considering a smaller increment $\gamma \ll \alpha$,

$$\frac{M}{EI} = \frac{\pi \gamma (\sin^2 \alpha) (\cos \alpha)}{h(1 + \gamma \sin \alpha \cos \alpha)} \quad (15)$$

Accordingly, the bending energy of the yarn segment is

$$U_{bend} = \frac{M^2 L}{2EI} = \frac{EI\pi^2\gamma^2(\sin^4\alpha)(\cos^2\alpha)}{2h^2(1+\gamma\sin\alpha\cos\alpha)^2} \frac{h}{\sin\alpha} \quad (16)$$

The bending energy per unit volume of HCYA is

$$u_{bend} = \frac{U_{bend}}{\pi R^2 h} = \frac{EI\pi\gamma^2(\sin^3\alpha)(\cos^2\alpha)}{2R^2 h^2(1+\gamma\sin\alpha\cos\alpha)^2} \quad (17)$$

where R is the radius of HCYA. As an approximate estimation for the present HCYA, we have

$$I = \frac{\pi r^4}{4}, \quad r = R\sin\alpha, \quad \frac{h}{2R} = \frac{\sin\alpha}{\cos\alpha} \quad (18)$$

where r is the radius of yarn. Further combining (17) and (18), comparing to the energy per unit volume of tension of PI fibers, and taking $\alpha \approx 57^\circ$ for the present HCYA,

$$\begin{aligned} u_{bend} &= \frac{\pi^2(\sin^3\alpha)(\cos^2\alpha)}{16} \left[\frac{E}{2} \gamma^2(\sin^2\alpha)(\cos^2\alpha) \right] \\ &= \frac{\pi^2(\sin^3\alpha)(\cos^2\alpha)}{16} u_{tension} \\ &\approx (0.108)u_{tension} \end{aligned} \quad (19)$$

Results show that the bending energy of yarn during the deformation is about 10% of the tensile energy of PI fibers. In comparison, the effect of bending could be approximately neglected for the present sample of HCYA.

Section 7. Calculation parameters for determining thermal-hardening effect

According to the benchmark in Table S2, the tensile modulus of PI varies within the range of 7787 – 1151 MPa when temperature increases from -50 °C to 150 °C, and the tensile modulus of PDMS varies within the range of 2 – 0.2 MPa when temperature increases from 20 °C to 180 °C. Taking the reference temperatures and modulus of PI and PDMS, material constants a_1 and a_2 can be obtained. Considering the Poisson's ratio of PDMS is 0.35, the shear modulus of PDMS is determined. By measurement on

the photos (Figure 4C~4D) and movie (movie S4), α increases with temperature, and θ is approximately a constant in the process of actuation. Finally, the parameters at 20°C and 100°C are estimated below.

T	α	θ	E_1 (MPa)	G_2 (MPa)	A_1	A_2
20 °C	$58.5^\circ \pm 1.5^\circ$	30°	5398	0.7324	32.2%	67.8%
100 °C	$54.5^\circ \pm 1.5^\circ$		2810	0.4074		

Section 8. Calibration of piezoresistive sensor adopted in pressure measurement of actuating fabric

The piezoresistive sensor was put into oven horizontally, followed by putting a load of 30g (approximate to the initial pressure of actuating fabric) on it. The temperature in oven was adjusted to 25, 40 and 60 °C, then recording the related value given by sensor, i.e. 30g, 34g and 43g. As the sensor has a round shape with diameter of 1.25cm, the resultant pressures were calculated as 2.396, 2.716, 3.434 kPa. Assuming that the influences of temperature and pressure on the output are independent, a linear curve of pressure-temperature was plotted accordingly as the baseline of pressure test of the actuating fabric. The relationship between the temperature and the output is given by

$$f(T) = 0.0284 * T - 0.71 \quad (20)$$

The applied pressure, $f(P)$, which is induced only by the constriction of fabric, is given by

$$f(P) = f(P, T) - f(T) \quad (21)$$

where the $f(P, T)$ is the recorded pressure affected by both pressure and temperature.

The detailed calibrating procedure is listed in Table S10.

Figures and legends:

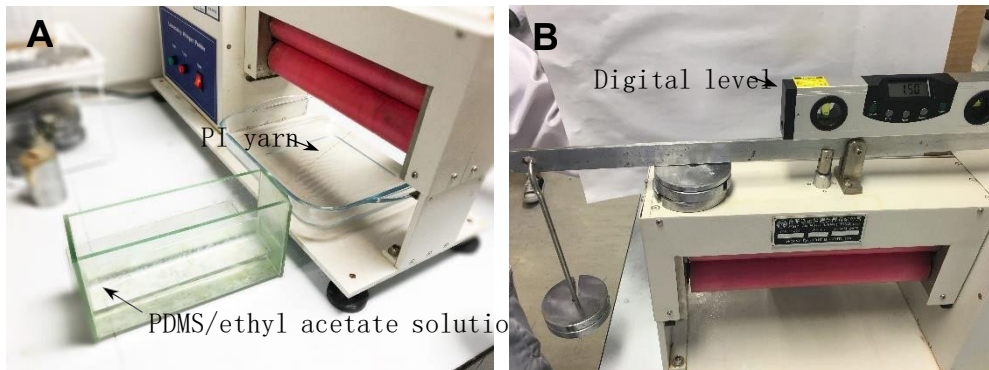


Figure S1 Processing system of padding method in (A) front view and (B) back view.

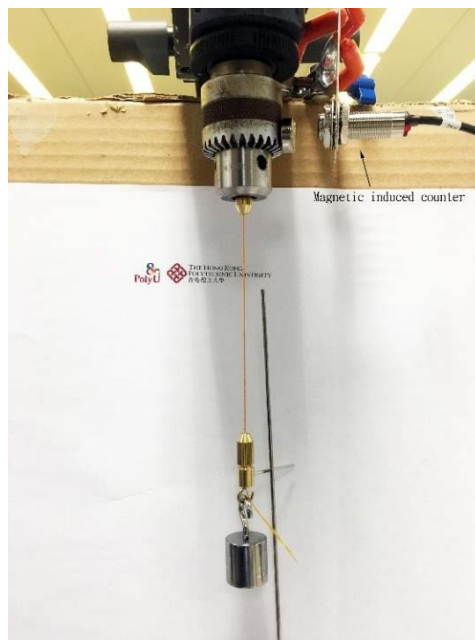


Figure S2 Experimental setup for fabricating thermally powered actuator

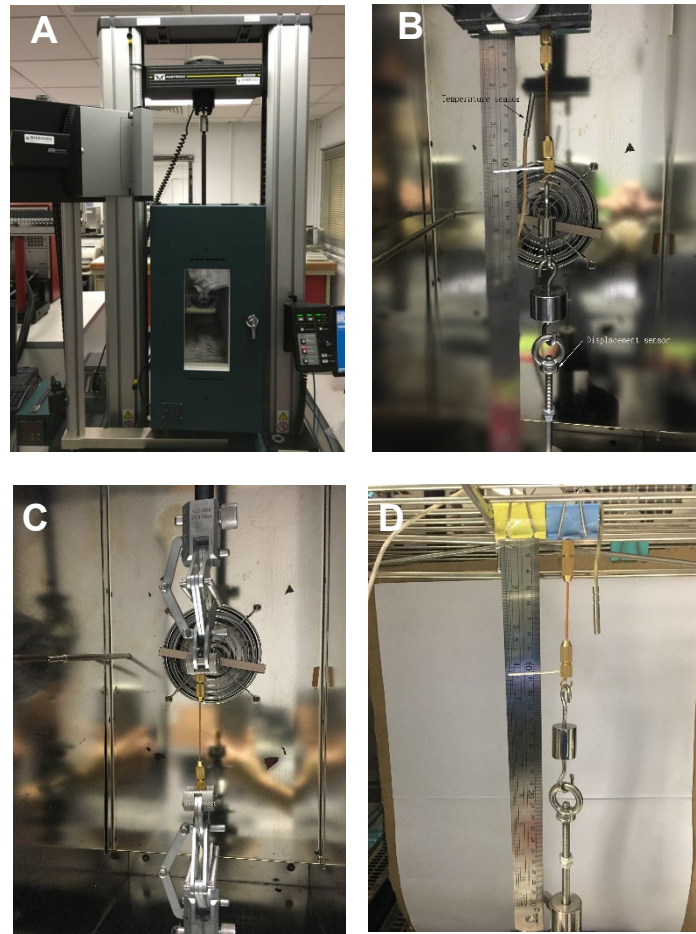


Figure S3 Thermomechanical test system. (A) Instron 5566 equipped with oven (B) Isotonic test system in Instron 5566 (C) Isometric and isothermal test system in Instron 5566 (D) Isotonic test system in climate chamber

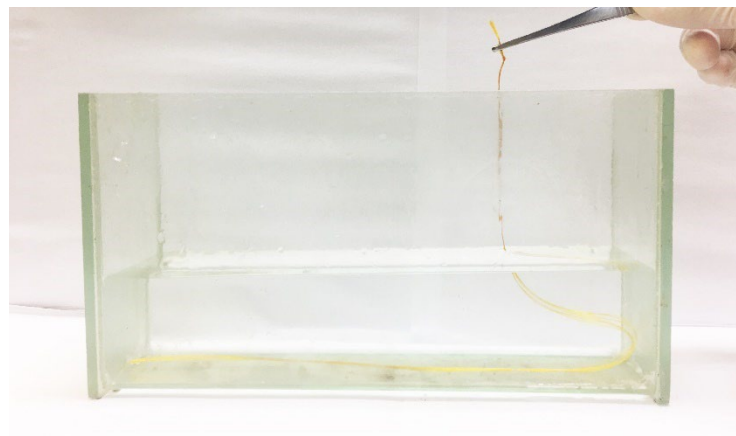


Figure S4 Impregnation by dip-coating method

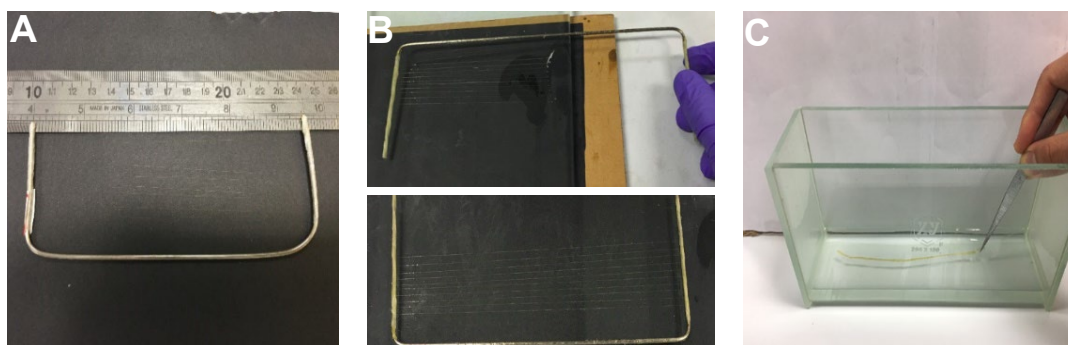


Figure S5 Impregnation process of glass board method. (A) Wind the monofilaments to metal framework (B) Dip-coating monofilaments with tension (C) Dip-coating the yarn made by combined coated monofilament without tension

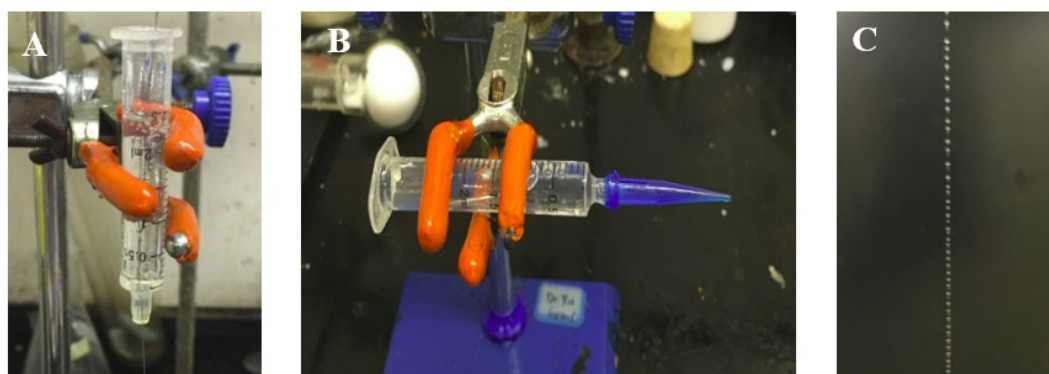


Figure S6 Impregnation process by nozzle-coating method. (A) Iron wire/PI monofilament goes through syringe half-filled with PDMS (B) Draw iron wire out of nozzle for coating PI monofilament (C) PDMS bead forms gradually after coating

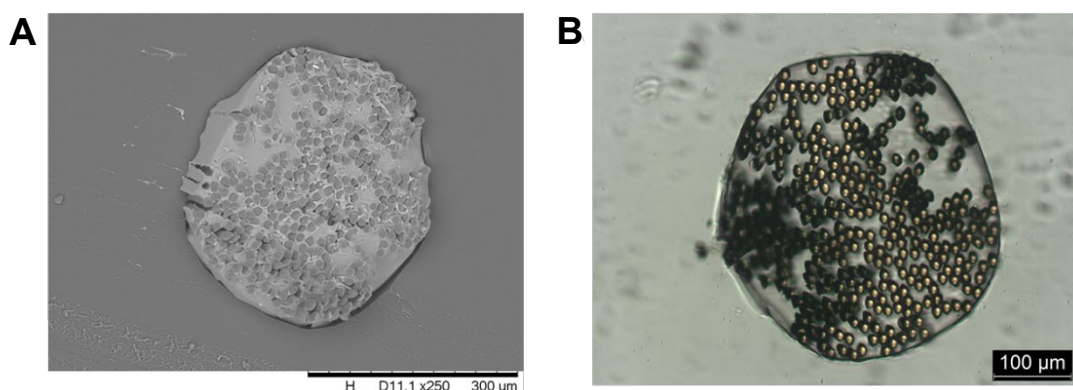


Fig S7 Cross-section view of 300f PI/PDMS composite yarn. (A) SEM photo (B) Leica DFC290 HD EM photo

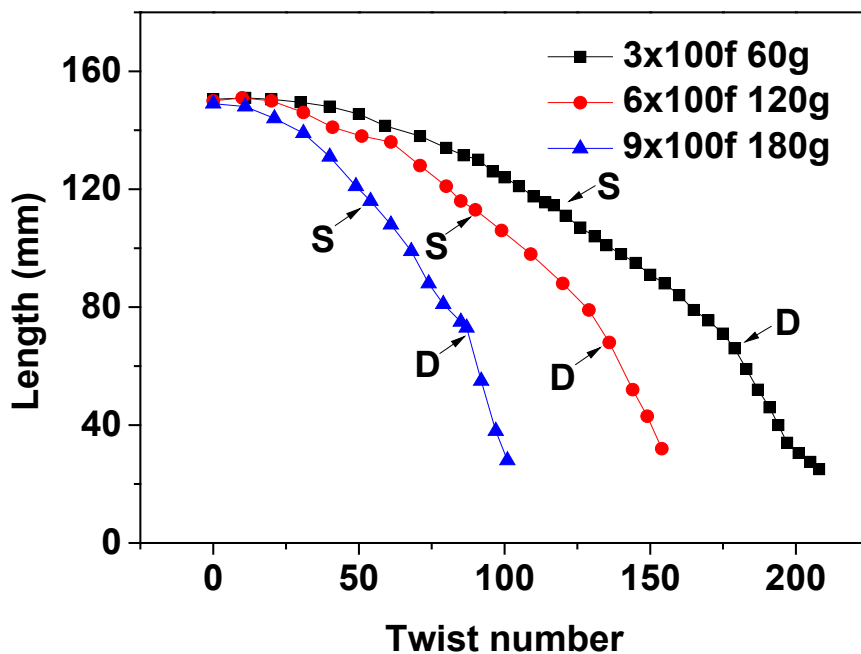


Figure S8 Twist curve of PI/PDMS composite yarns (S points: Single coils appear; D points: Double coils appear)

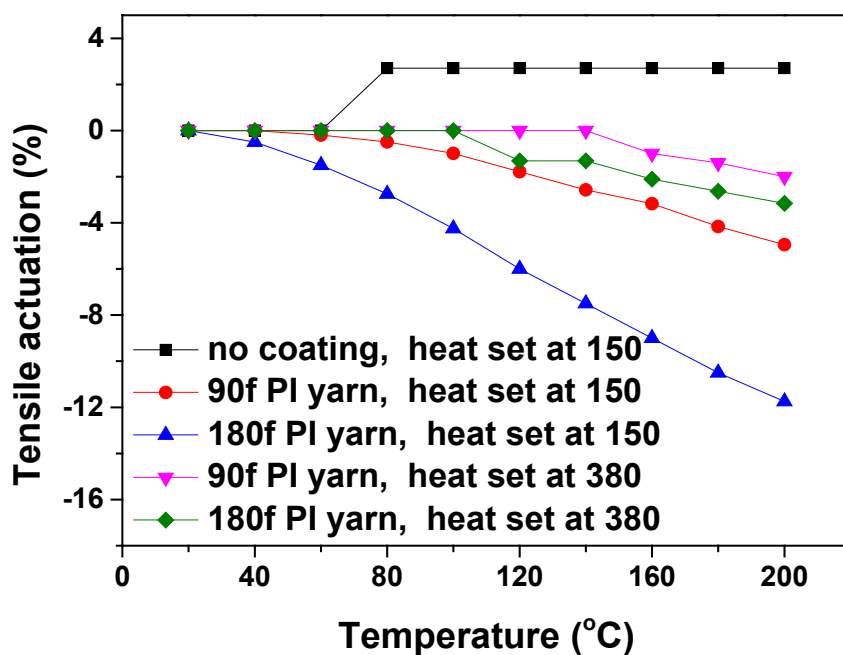


Figure S9 Thermal actuation of actuators with different filament number and heat-setting temperature. Note: The loads for all the actuators were 10 g.

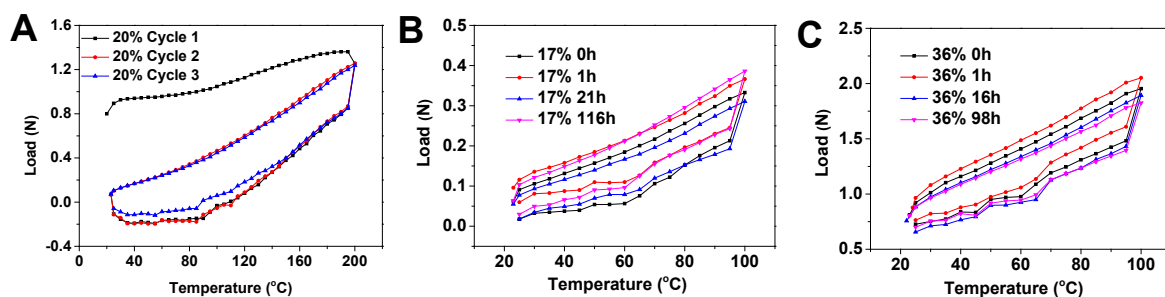


Figure S10 Isometric test of PI/PDMS HCYA. (A) Heat-setting cycles of PI/PDMS HCYA; (B) Repeatability after various time intervals between two cyclic isometric tests (pre-extension of 17%); (C) Repeatability after various time intervals between two cyclic isometric tests (pre-extension of 36%).

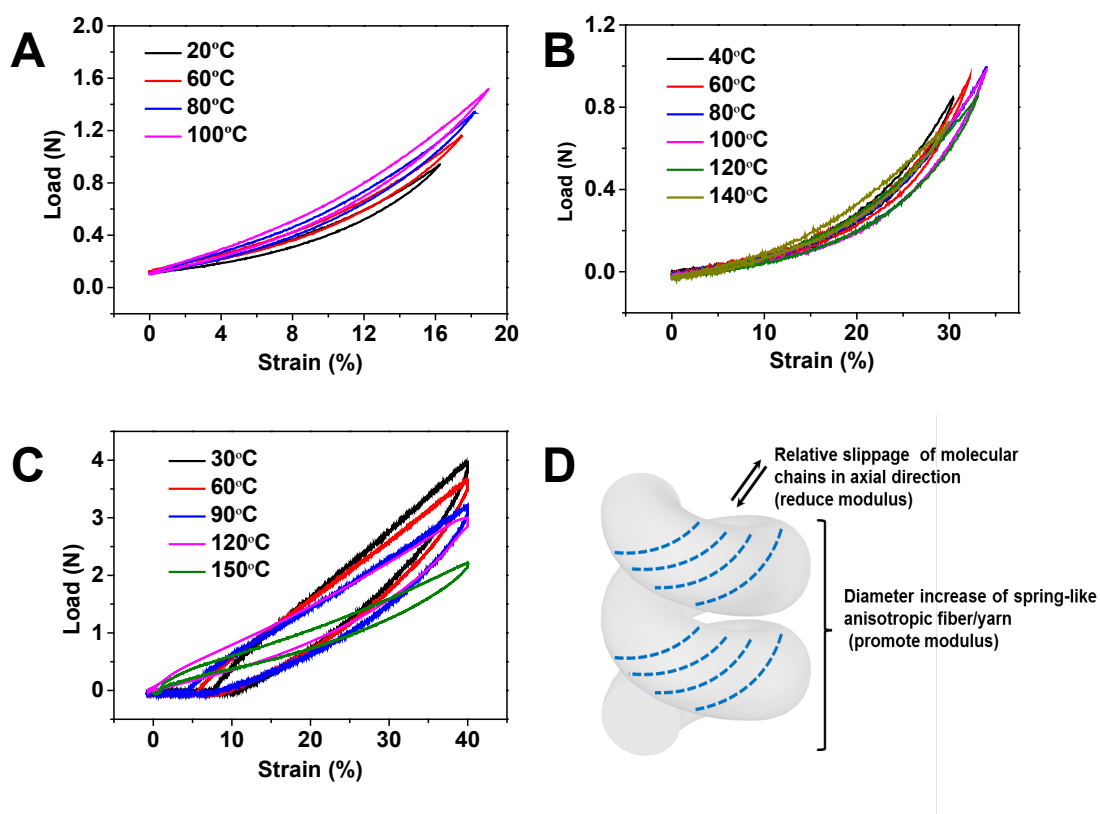


Figure S11 Isothermal tests of different actuators and related theoretical analysis. (A)-(C) Force-strain curves of 600f PI/PDMS HCYA, PET/PDMS HCYA and PET monofilament FCLA at various constant temperatures, respectively; (D) Schematic illustration of isothermal behavior of HCYAs.

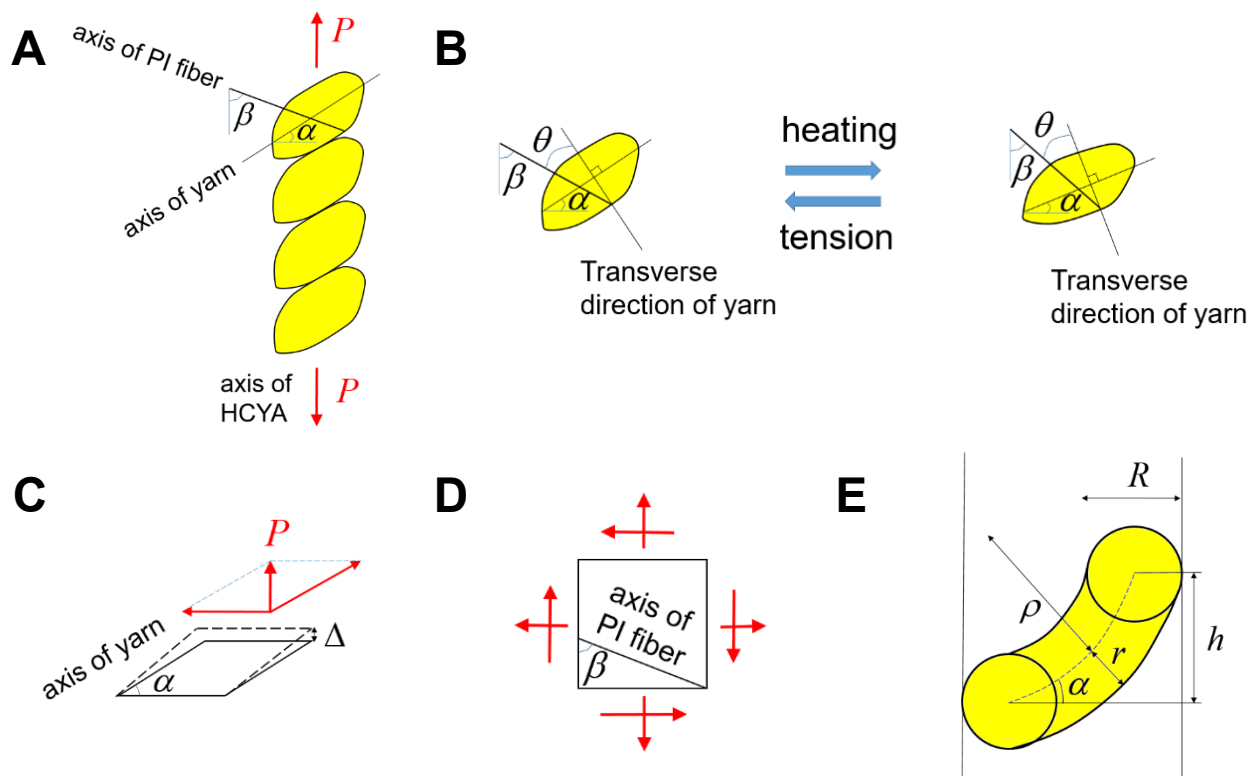


Figure S12 Configuration of HCYA. (A) Side view of HCYA under longitudinal tensile force P , where α is the angle between the axis of composite yarn and transverse direction of HCYA, β is the angle between the PI fiber and axis of HCYA; (B) State change of HCYA when heated or stretched; (C) Parallelogram element of yarn; (D) Shear of the anisotropic composite yarn; (E) Curved yarn segment in half-coil.

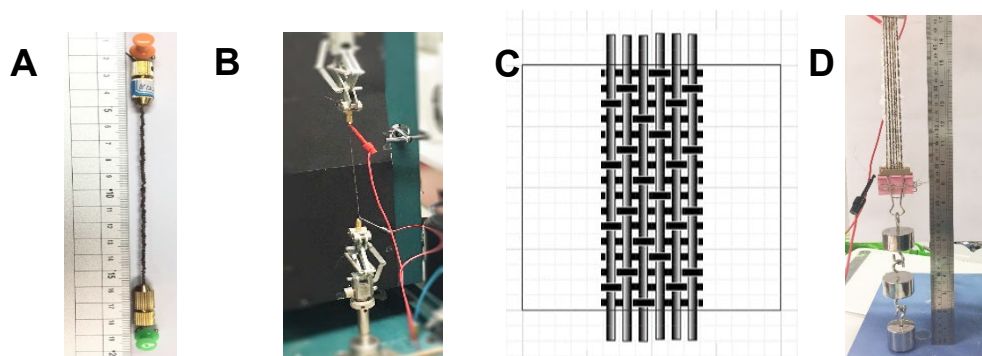


Figure S13 Electro-thermo-mechanical actuation and applications of 2-ply 300f PI/Cu/PDMS HCYA. (A) An PI/Cu/PDMS HCYA sample fixed at ends by two small clamps; (B) Isometric test set-up; (C) The sateen woven structure of PI/Cu/PDMS

actuating fabric; (D) Isotonic test set-up for the actuating fabric.

Tables:

Table S1 Properties of potential materials for fabricating HCYA based on composite yarn^[4-5]

Material	T _g (°C)	T _m (°C)	Ductile/Brittle Transition Temperature (°C)	safety	thermal expansion (10 ⁻⁶ °C ⁻¹)
Nylon	60	230	-65	Y	50-90
PET	78	265	-40	Y	59.4
Polyethylene	-110	141	-70	Y	108-200
Carbon nanotube	>2000	>2000	< -195	N	19-21
Carbon fiber	>2000	>2000	always	Y	<2
Polyimide	410	>500	-270	Y	30-60
Polydimethylsiloxane	-	-	-	Y	776
epoxy	-	-	-	-	45-65
paraffin	-	37	-	-	106-408

Table S2 Thermomechanical properties of composite yarns and their components

Item	PI filament	PDMS strip (0.41*1*12.5mm)	PI/PDMS 300f composite
------	-------------	-------------------------------	---------------------------

CTE (10^{-6}K^{-1})	-29.19 (-45-220 °C, 100f, axial, tension mode)	776 (-25-230 °C, tension mode)	424 (-50-180 °C, radial, compression mode)
Modulus (MPa)	7787~1150.8 (-50-150 °C, 1f, axial, tension mode)	2~0.2 (20~180 °C, tension mode)	110.0~36.8 (-60~180 °C, radial, compression mode)

Table S3. Influence factors of volume fraction

No.	Concentration of PDMS/ethyl acetate solution	Coating method	Coating times	Filament number	Volume Fraction of PDMS (%)
1	1:9	Dip-coat	once	100	5.7
2	1:5	Dip-coat	once	100	9.5
3	1:4	Dip-coat	once	100	10.7
4	1:4	Dip-coat	once	900	22
5	1:4	Pad	once	900	26.8
6	1:2	Pad	once	900	59.0
7	1:2	Pad	2 times	900	67.1
8	1:2	Pad	3 times	900	71.3
9	1:2	Pad	4 times	900	78.5
10	1:2	Pad	once	300	31.1
11	1:2	Pad	once	600	46.0

12	1:2	Pad	once	900	59.0
----	-----	-----	------	-----	------

Table S4 Single-level coil actuators heat-set under different temperature






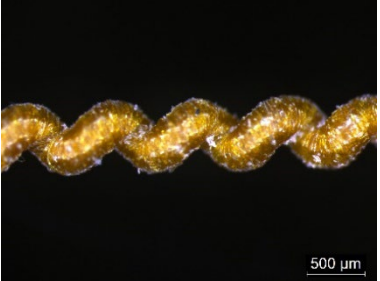
Heat-set temperature	150 °C	380 °C
90f		
180f		
270f		

Table S5 Isotonic behavior of 900f PI/PDMS HCYAs under different load

Load for 900f PI/PDMS actuator	Tensile actuation (%)	Specific work (J/kg)	Specific work capacity (J/(kg·°C))	R square
58.8 g	-17.7	57.2	0.38	0.99679
108.8 g	-16.8	114.1	0.76	0.99927
158.8 g	-16.2	158.9	1.06	0.99900

Note: Volume fraction of PDMS is 72.6%; Specific work of mammalian muscle is 38.6 J/kg. The specific work of the composite yarn actuators is higher. Temperature changes from -50 °C to 100 °C, i.e. $\Delta T = 150$ °C.

Table S6 Tensile actuation and specific work capacity of thermally powered **PI/Cu/PDMS** HCYAs of different filament number and coil level

PI/PDMS actuators heated from 20~25°C to 160°C		load for fabrication (g)	load for actuation (g)	Tensile actuation (%)	Specific work capacity (J/(kg·°C))
300f	single	8.7	28.7	11.0	0.66
	double	48.7	58.7	11.3	0.74
	Single & double	60	20	43.5	1.17
600f	single	18.7	58.7	19.5	0.59
	double	58.7	208.7	13.6	1.13
900f	single	18.7	108.7	14.6	0.73
	double	158.7	258.7	18.3	1.94

Table S7 Effect of volume fraction on tensile actuation and specific work capacity of **900f** PI/PDMS HCYAs

900f PI/PDMS actuator	Volume fraction of PDMS (%)	Fabric load (g)	Actuation load (g)	Extension rate (%)	ΔT (°C)	Tensile actuation rate (%)	Specific work capacity (kg·°C)
Dip-coat 1:4 single	74.6	18.7	108.7	23.2	133	14.6	0.73
Padding 1:2 single	54.0	18.7	108.7	14.1	140	8.2	0.59
Padding 1:4 single	35.9	18.7	108.7	5.2	140	5.0	0.35

Table S8 Isotonic tests of 300f and 600f PI/Cu/PDMS HCYA

PI/Cu/PDMS HCYA	300f	600f
Load (g)	78.7	100
length L (mm)	94	62
Length change ΔL (mm)	3.95	11.1
Power P (W), voltage U (V), current (I)	0.6, 3.87, 0.15	1.9, 5.95, 0.32
Tensile actuation (%)	-4.2	-17.9
Max. Actuation time (s)	30	33
Max. Temperature ($^{\circ}\text{C}$)	63.1	162
Energy conversion efficiency $\eta = mg \Delta L / UIt$ (%)	0.0175	0.0173

Table S9 Forming conditions of single-level & double-level coils

Load (g)	300f uncoated		300f coated		600f coated		900f coated	
	single	double	single	double	single	double	single	double
0.9	N	N	-	-	-	-	-	-
1.9	<u>Y</u>	N	-	-	-	-	-	-
8.7	Y	N	<u>Y</u>	<u>Y</u>	<u>Y</u>	N	<u>Y</u>	N
18.7	Y	N	Y	Y	Y	<u>Y</u>	Y	N
28.7	Y	N	Y	Y	-	-	-	-
68.7	-	-	Y	Y	-	-	-	-
78.7	-	-	Y	Y Break	-	-	-	-

108.7	Y	Break	Y	Y Break	Y	Y Break	Y	N
118.7	-	-	-	-	-	-	Y	<u>Y</u>
208.7	-	-	-	-	-	-	Y	Y
408.7	-	-	-	-	-	-	Break	-

Note: “Y” means the coil can form. “Y” means the coil can form under a minimum load. “N” means the coil cannot form. “Break” means the yarn was broken as the load was too heavy. “-” denotes “did not test”.

Table S10 Calibrating procedure of pressure of actuating fabric.

FTIR temperature /°C	Recorded load /g	Recorded pressure / kPa	Baseline pressure / kPa	Calibrated pressure / kPa
25.6	34	2.716	0.016	2.699
26.5	35	2.795	0.044	2.752
29.5	37	2.955	0.128	2.827
37.2	42	3.355	0.346	3.008
43.9	44	3.514	0.537	2.978
56.2	60	4.792	0.887	3.905

Movies:

Movie S1: Isotonic test of 600f PI/Cu/PDMS HCYA with a power of 1.9 W and voltage of 5.95 V

Movie S2: Grabbing of the robotic hand actuated by joule-heated PI/Cu/PDMS HCYA.

The parameters and performance are listed as follows:

Length: 24.2 cm Actuation: 2.9%

Temperature: 20~101 °C

Resistance: 13.5 Ω

Voltage: 8 V

Current: 0.594 A

Power: 4.8 W

Time: 30 s

Movie S3: Grabbing of the robotic hand actuated by joule-heated PI/Cu/PDMS HCYA under cold environment. The parameters and performance are as follows:

Length: 24.2 cm

Actuation: 2.9%

Ambient temperature: -50 °C

Resistance: 27.7 Ω

Voltage: 16 V

Current: 0.578 A

Power: 9.2 W

Time: 25 s

Movie S4: Morphology change of 600f PI/PDMS HCYA under air-heating. The parameters are as follows:

Fixed Length: 30 mm;

Initial temperature: 20 °C;

Maximum temperature: 106 °C

Time: < 8 s

Reference:

[1] T. H. Courtney, *Mechanical behavior of materials*. Waveland Press, Long Grove, IL, USA, 2005.

- [2] A. Cherubini, G. Moretti, R. Vertechy, M. Fontana, *AIP Adv.* **2015**, 5 (6), 067158.
- [3] J. E. Shigley, C. R. Mischle, *Mechanical Engineering–Design*. 5th ed.; McGraw-Hill, **1989**.
- [4] can be found under https://www.engineeringtoolbox.com/linear-expansion-coefficients-d_95.html.
- [5] can be found under <https://omnexus.specialchem.com/polymer-properties/properties/ductile-brittle-transition-temperature>.